이학 석사 학위 논문

Effect of human umbilical cord derived MSCs on bisphosphonate-related osteonecrosis of the jaw

비스포스포네이트 유래 턱뼈괴사증에 대한 인간 제대조직유래 중간엽 줄기세포의 치료효과

울 산 대 학 교 대 학 원

의 학 과

양 광 현

Effect of human umbilical cord derived MSCs on bisphosphonate-related osteonecrosis of the jaw

지 도 교 수　이 부 규

이 논문을 이학석사 학위 논문으로 제출함

2021 년 12 월

울 산 대 학 교 대 학 원

의　학　과

양 광 현

양광현의 이학석사학위 논문을 인준함

심사위원　　황 창 모　　인

심사위원　　이 부 규　　인

심사위원　　주 세 경　　인

울 산 대 학 교 대 학 원

2021년 12월

English Abstract

Background: Bisphosphonate-related osteonecrosis of the jaw (BRONJ) is a severe sequela caused by bisphosphonates (BPs), which are widely used to treat osteoporosis or other malignancies. However, the mechanism underlying BRONJ remains unclear. Recently, human umbilical cord-derived mesenchymal stem cells (hUC-MSCs) have been studied for treatment of diverse diseases and injuries. This study aimed to investigate the therapeutic effects of hUC-MSCs in BRONJ.

Methods: The therapeutic effects of hUC-MSCs were examined in rat bone marrow (rBM)-derived cells using cell viability, colony-forming, and real-time PCR assays and FACS for analyzing essential proinflammatory and bone regeneration markers in vitro. To demonstrate the in vivo therapeutic and adverse effects of transfused hUC-MSCs, micro-CT, H&E staining, IHC (Angiogenesis marker gene expression) staining, and parathyroid hormone (PTH)/calcium assay were conducted in a BRONJ-induced animal model.

Results: BP-induced cytotoxicity and inflammation in rBM-derived cells decreased, after co-culture with hUC-MSCs. The expression levels of bone regeneration markers (RUNX2, OSX, and BMP-2) significantly increased in BP-treated rBM-derived cells, after co-culture with hUC-MSCs. The BP-induced abnormal shift in RANKL/OPG expression ratio in rBM-derived cells was normalized by hUC-MSCs. Consistent with these in vitro results, transfused hUC-MSCs markedly decreased BRONJ and significantly healed injured mucosa in the BRONJ-induced animal model. The animals exhibited serious destruction of the kidney structure and

increases in serum PTH and calcium levels, which were significantly normalized by hUC-MSC transfusion.

Conclusions: hUC-MSCs exerted therapeutic effects on BRONJ in vitro and in vivo through their anti-cytotoxicity, anti-inflammatory activity and ability to recover bone regeneration.

Keywords: mesenchymal stem cells derived from human umbilical cord, bisphosphonates related osteonecrosis of the jaw, bone regeneration, hyperparathyroidism

Contents

List of Figures

Introduction

As the life span of humans has increased, more elderly patients suffer from various diseases, such as osteoporosis and malignancies related to bone metabolism [1]. For those patients, the periodic intake of bisphosphonates (BPs) is crucial to prevent bone resorption. However, some long-term users of BPs can develop bisphosphonate-related osteonecrosis of the jaw (BRONJ). BRONJ may cause serious health problems, primarily among elderly female patients, and the number of patients is growing worldwide, making BRONJ an urgent and critical public issue in the dental and medical fields.

BRONJ is defined as the necrotic exposure of maxillofacial or mandibular bone lasting more than 8 weeks in patients who have taken BPs without a history of radiation therapy administered to the jaw [2]. Until the occurrence of triggering events such as infection and exposure of the jawbone following surgery, as well as the concomitant use of immunosuppressive and chemotherapy drugs, BRONJ symptoms may be latent [2-4]. Based on accumulated evidence, scientists have hypothesized that the causes of BRONJ might be related to unbalanced bone metabolism due to osteoclasts, an inflammatory reaction due to infection, and suppression of angiogenesis in the lesion area [2-6]. Currently, surgeons and scientists attempt treating BRONJ using hyperbaric oxygen, platelet-rich plasma, low-level laser irradiation, and bone morphogenic proteins (BMPs) [5, 7, 8]. However, currently, there are no effective solutions for preventing and treating BRONJ.

Mesenchymal stem cells (MSCs) are well-known therapeutic agents with multilineage

differentiation and self-renewal capacities [9]. MSCs also secrete various growth factors and cytokines that are expected to promote tissue repair and exert anti-apoptotic effects [10-12]. The spectrum of local cytokines can be shifted from pro-inflammatory to anti-inflammatory by MSCs [13-15]. Previous studies examining the treatment of BRONJ using various MSC sources have been performed using different methods, including cell sheets, conditioned media, and intravenous injection [8, 16, 17].

The advantages of umbilical cord-derived mesenchymal stem cells (UC-MSCs) include ease of access, high proliferation potential, and low immunogenicity due to the immaturity of newborn cells [18, 19]. Furthermore, UC-MSCs possess a stronger ability to differentiate into osteoblasts than other types of MSCs, which can play a key role in bone regeneration [20]. Therefore, theoretically, severe damage to tissues caused by complex imbalanced immune reactions, such as those that occur in BRONJ, might be prevented by, or treated with, MSCs. Here, to determine the therapeutic effects of human umbilical cord-derived mesenchymal stem cells (hUC-MSCs) on BRONJ, we investigated the effect of hUC-MSCs on the proliferation/differentiation of rat bone marrow (rBM)-derived cells after zoledronate treatment (an in vitro BP-induced cell death model) and on bone repair ability (in an in vivo BRONJ-induced rat model) [8].

Materials and Methods

1. Animal experiment

We purchased 7-week-old female Sprague-Dawley (SD) rats, mean weight of 201 g (ranging from 182 to 217 g), from Orient Bio Inc. (Seoungnam, South Korea). According to the current international laws and policies (Guide for the Care and Use of Laboratory animals, NIH Publication No. 85-23, 1985, revised 1996), the experimental animals were handled and cared for in a facility certified under ISO9001 for this study. Briefly, the rats were raised in appropriated conditions, including a 12 h dark/light per day, a temperature of 24 ± 1°C in filtered air, and 50% ± 5% humidity. The animals were provided free access to a normal rodent diet and given water ad libitum. In addition, all experimental procedures were thoroughly reviewed and approved by the Institutional Animal Care and Use Committee (IACUC) of Asan Institute for Life Sciences, Asan Medical Center (NO: 2017-12-208). When conducting the animal experiments, we made an effort to minimize of the number of animals and their suffering caused by all procedures.

2. Preparation and cell culture of hUC-MSCs

hUC-MSCs were obtained from the Asan Stem Cell Center (Asan Medical Center, Seoul, South Korea). Briefly, IRB-approved human umbilical cords, with the vessels and amnions removed, were minced and digested using collagen A (Roche, Mannheim, Germany) in MEM (Invitrogen-Gibco, Carlsbad, CA) at 37°C with agitation. The cells were passed through a 70

μm mesh filter (BD Falcon, CA, USA) and centrifuged at 200 × g for 10 min. The isolated hUC-MSCs were cultured in DMEM-F12, supplemented with 10% FBS and an antibiotic-antimycotic mixture, at 37°C in a humidified 5% CO_2 incubator. We confirmed they were hUC-MSCs using BD FACSCanto II (BD Biosciences, CA, USA) and BD FACS Diva software 8.0.1 (BD Biosciences, CA, USA) using CD34 and CD45 as negative markers and CD37, CD90, and CD105 as positive markers of MSCs.

3. Preparation of rat bone marrow-derived cells (rBM-derived cells)

To simulate the in vitro conditions in vivo, we isolated rBM-derived cells from the femurs of wild type 7-week-old-female SD rats because immune cells and MSCs engage in cross-talk [23]. Generally, bone marrow-derived cells consist of two main stem cell populations and progenies: hematopoietic stem cells and mesenchymal stem cells. Therefore, we used the mixed cells to reproduce similar conditions in vivo.

rBM-derived cells were prepared using a modified previously described method [24]. DMEM-F12 (GE Healthcare Life Sciences Hyclone, Little Chalfont, UK), supplemented with 10% FBS (GE Healthcare Life Sciences Hyclone, Little Chalfont, UK), 10 nM 1α, 25(OH)2D3, and an antibiotic-antimycotic mixture (Gibco, MD, USA), was injected into the bone marrow using an 18-gauge syringe after the edges of each of femora were cut. The bone marrow cells were flushed out onto 100 mm2 culture dishes repeating several times and then incubated at 37℃ in 5% CO2/95% humidified air. After 3 d, the adherent cells were harvested with 0.25%

trypsin and 0.02% EDTA (Biological Industries, CT, USA), and the suspended cells were harvested by centrifugation. Suspended cells were stimulated with 50 ng/ml M-CSF for 7 d without changing the medium to differentiate them into immune cells. Before using the cells as rBM-derived cells, we mixed equal numbers of each cell type, using cells at passage number 3 to 6.

4. Co-culture of rBM-derived cells with hUC-MSCs

rBM-derived cells were seeded in 24 well culture plates at 1 × 105 cells/well, and hUC-MSCs were seeded in transwells at 2 × 104 cells/well. The cells were cultured at 37℃ in 5% CO2/95% humidity. The next day, the cell media were changed to serum-free DMEM-F12 containing an antibiotic-antimycotic mixture and 10 nM 1α, 25(OH)2D3. Then, the cells were co-cultured for 24 h to allow communication between them. The cells were then treated with 100 μM zoledronate (Zol) for various times.

5. Cell viability assay

The cell counting assay kit-8 (CCK-8; Dojindo Laboratories, Kumamoto, Japan) was used to evaluate the viability of rBM-derived cells treated with Zol (Sigma-Aldrich, St. Louis, MO, USA). After co-culturing with hUC-MSCs, rBM-derived cells were treated with 100 μM Zol for 24 h, 48 h, or 72 h. The cell viabilities were evaluated with a CCK-8 assay kit according to the manufacturer's instructions. Absorbance was measured at 450 nm with an ELISA

microplate reader (Sunrise; Tecan Austria GmbH, 5082 Grödig, Austria). Cell viabilities are presented as a percentage of the control for each time.

6. FACS analysis

The rBM-derived cells were characterized using BD FACSCanto II (BD Biosciences, CA, USA) and BD FACS Diva software 8.0.1 (BD Biosciences, CA, USA) to observe the MSC surface markers. Briefly, cells were incubated with anti-CD29 (BD Biosciences, CA, USA; catalog No. 555005), anti-CD34 (MyBioSource, Inc., CA, USA; catalog No. MBS438123), anti-CD45 (BD Biosciences, CA, USA; catalog No. 559135), anti-CD73 (BD Biosciences, CA, USA; catalog No. 551123), anti-CD90 (BD Biosciences, CA, USA; catalog No. 554897), and anti-CD105 (Abcam, Cambridge, United Kingdom; catalog No. ab156756) for 40 min at 4o C. Stained cells were analyzed using the Flowing software (http://flowingsoftware.btk.fi)

7. Colony assay

From each experimental group, the P2 rBM-derived cells were suspended in α-MEM supplemented with 10% FBS and plated in 100-mm culture dishes at the density of 1000 cells/dish. The colonies were counted using Crystal Violet stain at 3 weeks after culture.

8. Osteogenic differentiation

For osteogenic differentiation, cells at passage 2 of the culture were plated in 12-well plates at densities of 2 x 103 cells/cm2. After 24 h, the cells were incubated in the differentiation medium for each lineage. The osteogenic medium consisted of α-MEM supplemented with 10% FBS, 10 mM β-glycerophosphate, 100 nM dexamethasone, and 50 μg/ml ascorbate-2 phosphate (Sigma-Aldrich, MO, USA). After 3 weeks of differentiation, cells were stained with Alizarin red S to observe the degree of mineralization. For each group, the qPCR was also performed to confirm the osteogenic markers [runt-related transcription factor 2 (RUNX2), osterix (OSX), bone morphogenic protein 2 (BMP-2), and glyceraldehyde 3-phosphate dehydrogenase (GAPDH)] (Table 1).

Table 1 Primer sequences

Primer	Sequence (5′-3′)
IL-1β	F-CACCTCTCAAGCAGAGCACAG
	R-GGGTTCCATGGTGAAGTCAAC
IL-6	F-TCCTACCCCAACTTCCAATGCTC
	R-TTGGATCTTGGTCCTTAGCC
TNF-α	F-AAATGGGCTCCCTCTCATCAGTTC
	R-TCTGCTTGGTGGTTTGCTACGAC
OPG	F-CGAAGAGGCATTCTTCAG
	R-TCTGCATTCACTTTGGTC
RANKL	F-GTCGTTAAAACCAGCATC
	R-CCTGACCAGTTCTTAGTG
Runx2	F-TCTGTCCCGTCACCTCCATC
	R-ACAAGTTAGCGAAGTGGCCG
OSX	F-GGAGGTTTCACTCCATTCCA
	R-TAGAAGGAGCAGGGGACAGA
BMP-2	F-GAGTTTGAGTTGAGGCTGCTC-
	R-TGAGTCACTAACCTGGTGTCC′
GAPDH	F-GTTCCAGTATGACTCTACC
	R-TCACCCCATTTGATGTTA

9. Real-time reverse-transcriptase polymerase chain reaction (RT-PCR)

After co-culture for 24 h, rBM-derived cells were stimulated with 100 μM Zol for 2 d to analyze pro-inflammatory cytokines (IL-1β, lL-6, TNF-α) and osteogenic markers (Runx2, OSX, BMP-2). To evaluate of RANKL and OPG mRNA expression levels, the cells were stimulated with 50 μM Zol for 2 or 5 d. Total RNA was isolated from the harvested cells using a Pure Link™ RNA Mini Kit (Ambion, CA, USA) according to the manufacturer's protocol. Total RNA was used to synthesize cDNA with the SuperScript II cDNA synthesis kit (Invitrogen, CA, USA). Then, the transcribed cDNA was used for amplification with specific primers for IL-1β, IL-6, tumor necrosis factor alpha (TNF-α), osteoprotegerin (OPG), receptor activator of nuclear factor kappa-B ligand (RANKL), runt-related transcription factor 2 (RUNX2), osterix (OSX), bone morphogenic protein 2 (BMP-2), and glyceraldehyde 3-phosphate dehydrogenase (GAPDH) (Table 1). The RNA expression levels were analyzed with a 7900 real-time PCR system (Applied Biosystems, CA, USA) using Power SYBR Green PCR Master Mix (Applied Biosystems, CA, USA).

10. Animal study design

To explore the effect of hUC-MSCs on a BRONJ-induced animal model, the animals were divided into three groups: a control group (n=10), BPs-treated group (n=10), and hUC-MSC group (n=10). The BRONJ-induced animal model was prepared using a slightly modified method from previous studies [8, 14, 17]. To induce BRONJ in SD rats, the animals were

administered Zol (66 μg/kg/week; Novartis Pharma Stein AG., Schaffhauserstrasse 4332 Stein, Switzerland) and dexamethasone (Dex; 5 mg/kg/d; Yuhan, Seoul, Korea) subcutaneously for 4 weeks. Two weeks after subcutaneously injection, maxillary molars were extracted under general anesthesia with Alfaxan (10 mg/kg; Jurox, Rutherford NSW 2320, Australia) and Rompun (10 mg/kg; Leverkusen, Germany). In the hUC-MSCs group, the cells (1 × 106 cells in 1 × normal saline) were administered intravenously at 5 and 6 weeks

11. Serum assay (parathyroid hormone and calcium)

Before sacrifice, the blood from each rat was obtained from the heart while under general anesthesia with Alfaxan and Rompun, and then, whole blood cells were separated using Vacutainer SST™ Ⅱ Advanced (BD, Plymouth, UK) at 1000 × g for 15 min at 4℃. The serum concentrations of calcium and parathyroid hormone (PTH) were measured using a calcium assay kit (Abnova, Taipei, Taiwan) and parathyroid hormone ELISA kit (MyBioSource, CA, USA). All procedures were performed according to the manufacturer's instructions.

12. Radiographic analysis (in vivo micro-computed tomography)

All animals were scanned at 5 and 8 weeks (as shown in Fig. 3B) using SkyScan 1172 high-resolution micro-CT (SkyScan N.V., Kontich, Belgium) to obtain radiographic images of the jaw bone. The scan settings were as follows: energy of 70 kV, intensity of 357 μA, resolution of 12.51 μm pixels, and rotation step size of 0.7°. A calibration scan was conducted using

SkyScan CT-Analyser software and a modified cone-beam algorithm with 0.027 mm × 0.027 mm × 0.027 mm isotropic voxel spacing. All procedures were conducted following the recommendations of the manufacturer.

To analyze the bone volume in the BRONJ-induced defect site, we assigned the region of interest (ROI) to include the alveolar bone from the first molar to the second molar. The slice segment selected in the ROI was measured by three-dimensional analysis using CTAn software (Bruker, Karlsruhe, Germany) to measure quantitative bone volumes.

13. Tissue processing and histological analysis

After sacrifice, the maxillae were taken and fixed in 4% paraformaldehyde for 1 week and decalcified in Claci-Clear Rapid (National diagnostics, GA, USA) at room temperature for 3 d prior to immersion in paraffin to analyze the histology of the specimen. The paraffin-embedded blocs were cut trans-axially to create 5-μm-thick slices using a microtome (Leica Microsystem, Wetzlar, Germany), and the sections were stained with hematoxylin (Sigma-Aldrich, St. Louis, MO, USA) and eosin (Sigma-Aldrich, St. Louis, MO, USA) for histological observation. All histological images were obtained with a BX53 Upright Microscope (Olympus, Tokyo, Japan) equipped with a digital camera (DP73; Olympus) connected to a computer monitor.

14. Statistical analyses

To analyze multiple group comparisons, statistical analyses were performed using one-way analysis of variance (ANOVA) followed by Bonferroni's post hoc test to compare the means of the groups. Comparisons between the BPs-treated and hUC-MSCs groups were analyzed using two-tailed Student's t-test. All statistical analyses were performed with Prism 7 for Windows (GraphPad Software, La Jolla, CA, USA, www.graphpad.com). The threshold value for statistical significance was set at 0.05, and P-values are noted as follows: a single asterisk for values between 0.05 and 0.01, two asterisks for significance ranging from 0.01 to 0.001, and three asterisks for values below 0.001.

Results

Effects of hUC-MSCs on the cell proliferation

The proliferation of the rBM-derived cell was determined by the total cell number and the CCK-8 assay. For counting the total cell number, 1x104 cells/well were cultured in a 12-well culture plate, and the whole-cell amount was calculated at 24 h, 72 h, and 120 h. At 120 h of culture, the BP-treated group showed an increase up to 4 folds, while hUC-MSC group showed an increase up to 8 folds, and the control group showed an increase up to 12 folds. The results of the CCK-8 assay were consistent. The number of viable cells in the hUC-MSC group was higher than that in the BP-treated group. However, the viability of both groups was lower than the control group. The assay was performed at 24 h, 48 h, and 72 h of the culture (Fig. 1 a,b)

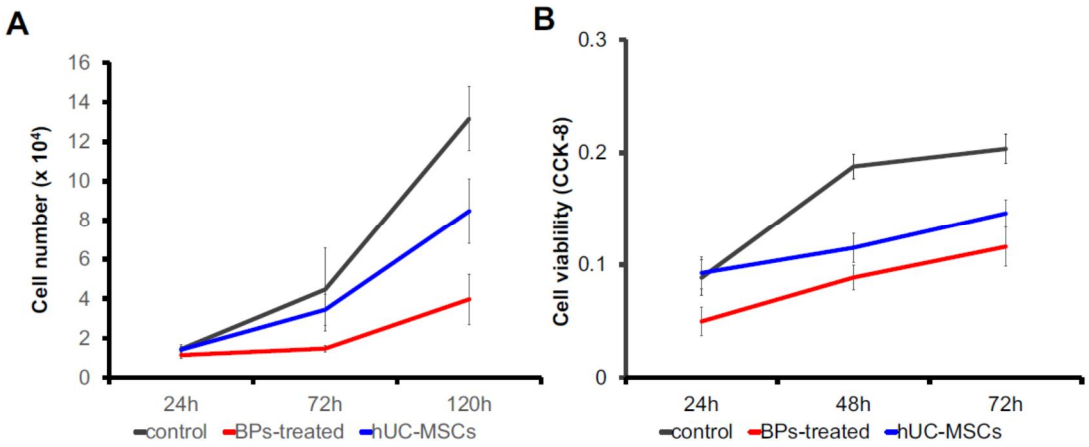

Fig. 1. Flow cytometric analysis of mice Th1/Th2/T17 phenotyping kit and effects of CMIT/MIT exposure in AD mice model. Statistical significance was determined with one-way analysis of variance (ANOVA). (*P < 0.05, **P < 0.01, ***P < 0.001).

Effects of hUC-MSCs on the characterization of rBM-derived cells

The expression of stem cell markers was analyzed in rBM-derived cells after treatment with hUC-MSCs compared to that in the non-treated group. Figure 5 c showed the high expression of CD29, CD73, CD90, and CD105, and no significant differentiation was observed in all groups. The expression of CD34 and CD45 increased after treatment with BP and hUC-MSCs in comparison with that in the control group (Figure 1b).

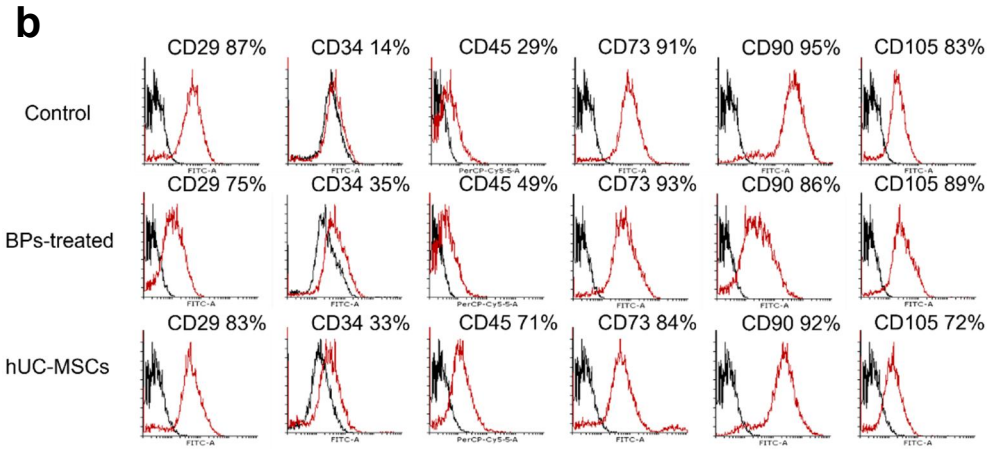

Fig. 1. The effect of hUC-MSCs on stem cell characterization of rBM-derived cells. **B** A high expression of CD29, CD73, CD90, and CD105 was observed, and there is no significant difference among all groups. Other, CD34 and CD45 increased after BP and hUC-MSC treatments, in comparison with those observed in the control group. (ANOVA). (*P < 0.05, **P < 0.01, ***P < 0.001).

Effects of hUC-MSCs on colony-formation and osteogenesis in rBM-derived cells

Control, BP-treated, and hUC-MSC groups were positive in the colony-forming assay (21.33 ± 2.05 colonies, 8.00 ± 1.63 colonies, and 15.33 ± 1.25 colonies, respectively) (Figure 1 c). Cells cultured in the osteogenic medium for 21 days showed alizarin red S-positive calcium deposits (2.43 ± 0.06, 0.73 ± 0.09, and 1.65 ± 0.07, respectively) (Figure 1 d). This result suggested that osteoblasts generated in hUC-MSCs.

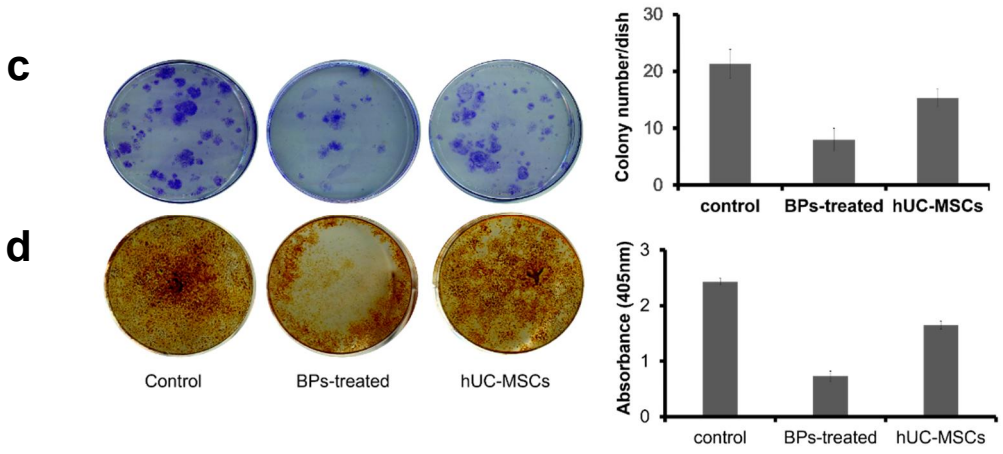

Fig. 1. The effect of hUC-MSCs on cell proliferation, stem cell characterization, colony formation, and osteogenic differentiation of rBM-derived cells. **C** Control, BP-treated, and hUC-MSC groups were positive in the colony-forming assay (21.33 ± 2.05 colonies, 8.00 ± 1.63 colonies, and 15.33 ± 1.25 colonies, respectively). **D** Osteogenic differentiation was evaluated via alizarin red-S staining. Cells cultured in the osteogenic medium for 21 days showed alizarin red S-positive calcium deposits (2.43 ± 0.06, 0.73 ± 0.09, and 1.65 ± 0.07, respectively) .

The effects of hUC-MSCs on pro-inflammatory cytokine expression in rBM-derived cells

Furthermore, we examined the effect of hUC-MSCs on BP-induced inflammatory responses in rBM-derived cells. After BP treatment, rBM-derived cells showed significantly increased expression of pro-inflammatory cytokines, 7.1-fold for IL-1ß, 1.4-fold for IL-6, and 6.4-fold for TNF-α compared to that in the control group. However, those cytokine levels were significantly decreased by co-culturing with hUC-MSCs, which might indicate an anti-inflammatory effect of hUC-MSCs (Fig. 2 a-c).

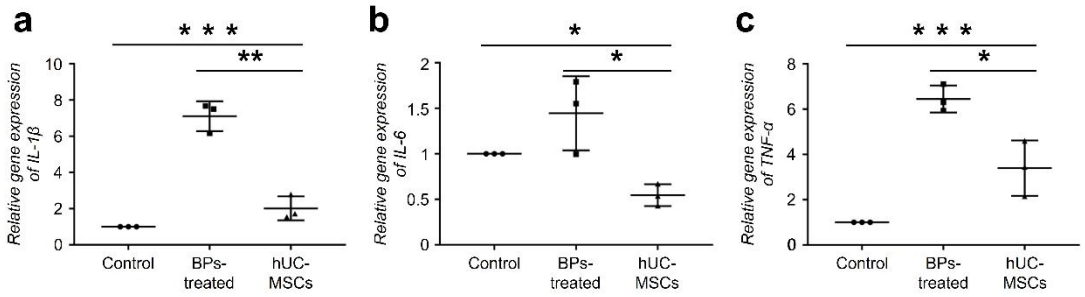

Fig. 2. The effects of hUC-MSCs on pro-inflammatory cytokine expression in rBM-derived cells. **A–C** The effects of hUC-MSCs on the pro-inflammatory cytokine expression were observed via evaluation of IL-1ß, IL-6, and TNF-a expression. After BP treatment, rBM-derived cells showed significantly increased expression of pro-inflammatory cytokines, such as 7.1-fold for IL-1ß, 1.4-fold for IL-6, and 6.4-fold for TNF-a, compared to that in the control group. However, those cytokine levels were drastically decreased in the hUC-MSC-treated group. (n = 10 per group) (ANOVA). (*P < 0.05, **P < 0.01, ***P < 0.001).

Effects of hUC-MSCs on the expression levels of osteoblast differentiation markers

rBM-derived cells treated with BPs showed no significant alteration in the RUNX2 expression level. However, in the hUC-MSC group, RUNX2 expression significantly increased to 5-fold compared to that in the control (Fig. 2 d). The OSX expression level in BP-treated cells decreased to 0.7-fold compared to that in control; however, the level in the hUC-MSC group significantly increased to 2.8-fold (Fig. 2 e).

Furthermore, we investigated the differences in bone morphogenetic protein 2 (BMP-2) expression levels caused by hUC-MSCs. When rBM-derived cells were treated with 100 μM Zol, BMP-2 expression in the cells did not change. In contrast, the level of BMP-2 expression in the hUC-MSC group significantly increased to approximately 2.9-fold compared to that in the BP-treated group (Fig. 2 f).

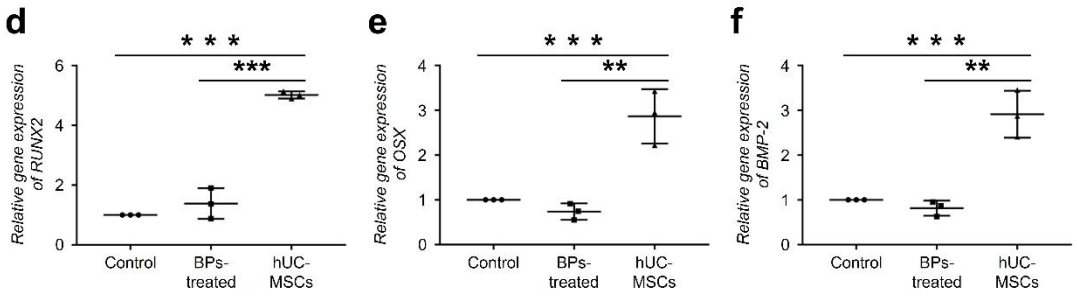

Fig. 2. The effects of hUC-MSCs on pro-inflammatory cytokine expression in rBM-derived cells. D–F The RANKL expression level drastically increased to 11.2-fold, and the RANKL/OPG ratio increased to 8.4-fold, on day 5 compared to those in the control. However, in the hUC-MSC group, the RANKL and OPG expression levels in the cells were drastically normalized. (n = 10 per group)) (ANOVA). (*P < 0.05, **P < 0.01, ***P < 0.001).

Changes in the expression levels of RANKL and OPG induced by hUC-MSCs

Here, we investigated RANKL and OPG expression levels on days 2 and 5 after the culture. On day 2, the expression levels of RANKL and OPG in the BP-treated group significantly increased to 2.2- and 7.2-fold compared to those in the control group, respectively. However, the RANKL/OPG ratio decreased to 0.3-fold compared to that in control (Fig. 3 a-c). The RANKL expression level significantly increased to 11.2-fold and the RANKL/OPG ratio increased to 8.4-fold on day 5, compared to those in the control (Fig. 3 d-f). However, in the hUC-MSC group, RANKL and OPG expression levels in the cells were drastically normalized.

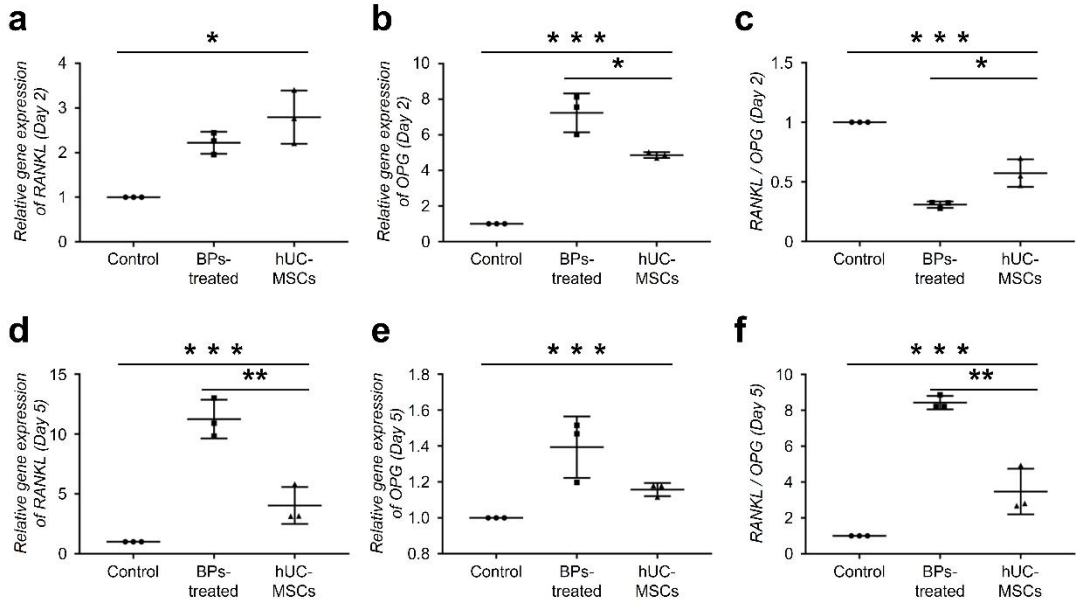

Fig. 3 Change in the expression levels of RANKL and OPG induced by hUC-MSCs. Expression levels of RANKL and OPG were evaluated on days 2 and 5 after culture. A–C On day 2, the expression levels of RANKL and OPG in the BP-treated group significantly increased to 2.2- and 7.2-fold compared to those in the control group, respectively. However, the RANKL/OPG ratio decreased to 0.3-fold compared to that in control. (D–F) The RANKL expression level drastically increased to 11.2-fold, and the RANKL/OPG ratio increased to 8.4- fold, on day 5 compared to those in the control. However, in the hUCMSC group, the RANKL and OPG expression levels in the cells were drastically normalized. (n = 10 per group) (ANOVA). (*P < 0.05, **P < 0.01, ***P < 0.001).

Inhibition of BRONJ by hUC-MSCs in a BRONJ-induced animal model.

To analyze the morphological changes in maxillae, all animals were subjected to micro-CT scanning 5 and 8 weeks after the first injection of Zol and Dex. BRONJ induced morphological changes were observed in the BPs-treated and hUC-MSCs groups from 5 weeks. As shown in Fig. 1, the rats with BRONJ showed osteolytic lesions, including sequestrum formation on the maxillae, unlike the control animals (Fig. 4 a, b, d and e). At 8 weeks, the sequestra disappeared or decreased in the BPs-treated group since the dislodgement of the sequestra and expansion of a destructed area (Fig. 4 b and e). The hUC-MSCs group showed smaller destruction of the area compared to the BPs-treated group, at 8 weeks (Fig. 4 c and f). In coronal view, osteolytic bone of the BPs-treated group was also observed as shown in the sagittal view (Fig. 4 I and k). As shown phenomenon in sagittal views, the coronal views revealed that the hUC-MSCs treated group showed less destruction on the maxillae bone than the BPs-treated group at 8 weeks (Fig. 4 i to l). In addition, the bone volume demonstrated that hUC-MSCs treated group was decreased bone destruction in maxillae (Fig. 4 m and n)

The bone volumes of all animals were measured at 5 and 8 weeks. The volume in BRONJ-induced rats decreased to approximately 22.0 mm3 on average, but the bone volume in control rats was 23.9 mm3 (Fig. 4 m). At 8 weeks, the bone volume in BRONJ-induced rats further decreased to 20.1 mm3. However, the bone volume in hUC-MSC-transfused rats significantly increased to 23.6 mm3 (Fig. 4 n).

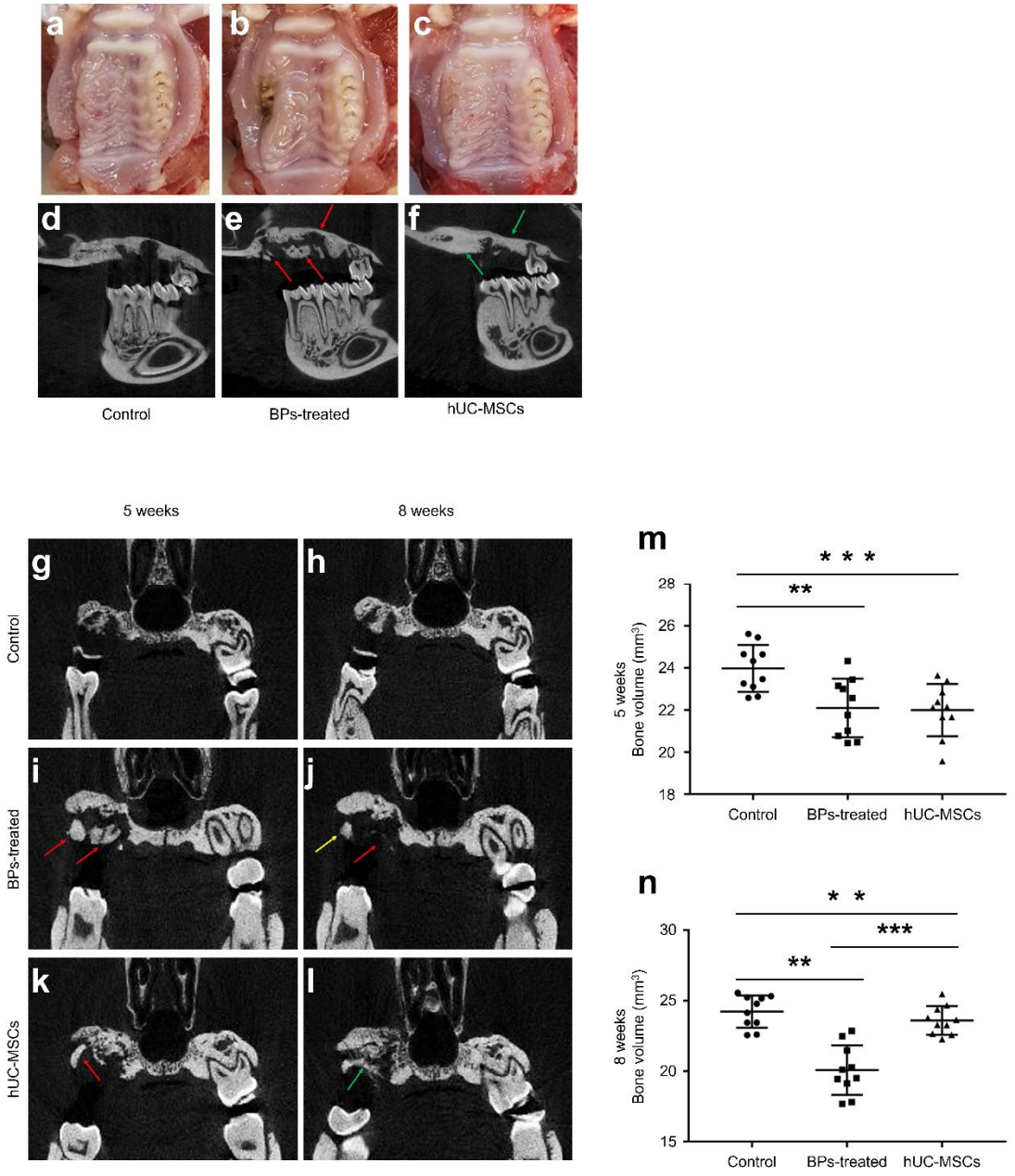

Fig. 4 A–F Inhibitory effect of hUC-MSCs on BRONJ in an animal model. Gross images (A–C) and sagittal microCT images (D– F) observed at 8 weeks.

Destruction of the maxillae bone observed in the hUC-MSC-treated group (C, and F) was less than that observed in the BP-treated group (B, and E). There was no maxillae bone in the control group (A, and D). (G) and (H) are coronal views of the control jawbone, observed at 5

or 8 weeks. At 5 weeks, the BP-treated (I) and hUC-MSC (K) groups showed bone sequestra (red arrows) and fistulae induced by BRONJ. At 8 weeks, the sequestra were collapsed (red arrow) and dislodged (yellow arrow) in the BP-treated group (J). However, as shown by the green arrow, the maxilla bone of the hUCMSC group (I) was regenerated in the destructed area. (M) and (N) measurement of the bone volumes in the alveolar bone from the first molar to the second molar of the maxillae. The graphs indicate bone volumes observed at 5 weeks (G) or 8 weeks (H). n = 10 per group. (ANOVA). (*P < 0.05, **P < 0.01, ***P < 0.001).

Suppression of an increase in serum PTH, calcium, and IL-6 by transfused hUC-MSCs in a BRONJ-induced animal model

The BP-induced decrease in osteoclasts and renal injury could cause hypocalcemia, which would subsequently induce the secretion of PTH from parathyroid glands. As shown in Fig. 2 a, after two injections of hUC-MSCs, the average level of PTH in the control group was 64.2 pg/ml. However, the BRONJ-induced animal models showed increased values up to 253 pg/ml, and the average serum PTH concentration was 171.1 pg/ml. The hUC-MSC-transfused group showed decreased PTH levels of 105.9 pg/ml, on average. We also investigated blood calcium levels in the experimental animals. The average blood calcium levels were approximately 10.7 mg/dl, 15.2 mg/dl, and 13.9 mg/dl in the control group, BP-treated group, and hUC-MSC-transfused group, respectively (Fig. 5 b).

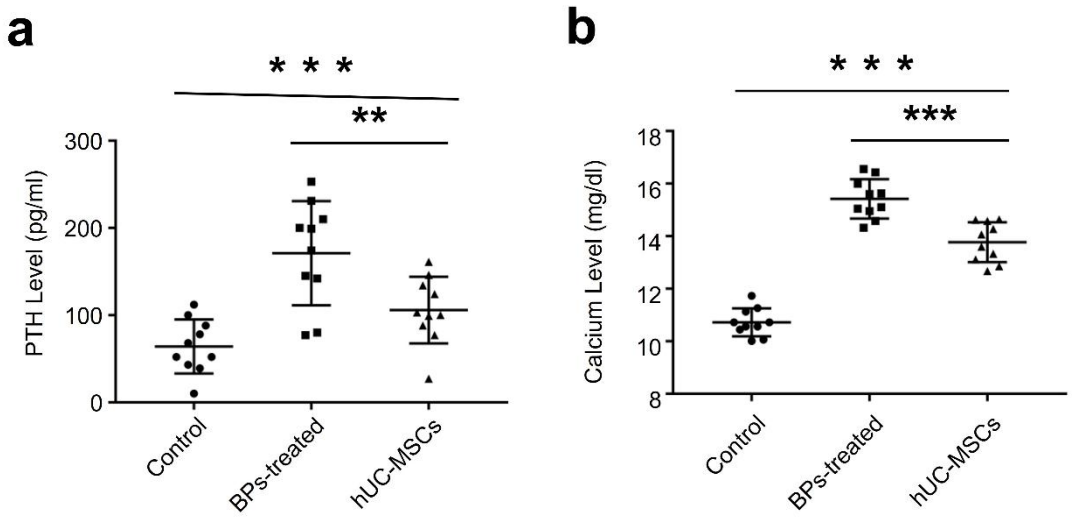

Fig. 5 Suppression of an increase in the serum PTH and calcium levels by transfused hUC-MSCs in a BRONJ-induced animal model.

A Expression of PTH in the hUC-MSC-treated group was lower than that in the BP-treated group, but it was higher than that in the control group. B Levels of calcium in the hUC-MSCtreated group were lower than those in the BP-treated group, but they were higher than those in the control group. (ANOVA). (*P < 0.05, **P < 0.01, ***P < 0.001).

Oral mucosal structure and other organs by hUC-MSCs

We performed H&E staining, after sacrifice, to analyze the recovery of the overlying oral mucosal integrity induced by hUC-MSCs in the BRONJ-induced animal model. In the BP-treated group, mucosal tissue structure was discontinuous and destroyed, as shown in Fig. 6A. However, in the hUC-MSC-transfused group, the overlying oral mucosa on the tooth extracted site was similar to that observed in the It appears, to reduce repetitive text, this should simply be ‘‘control’’ group (Fig. 6A–C)

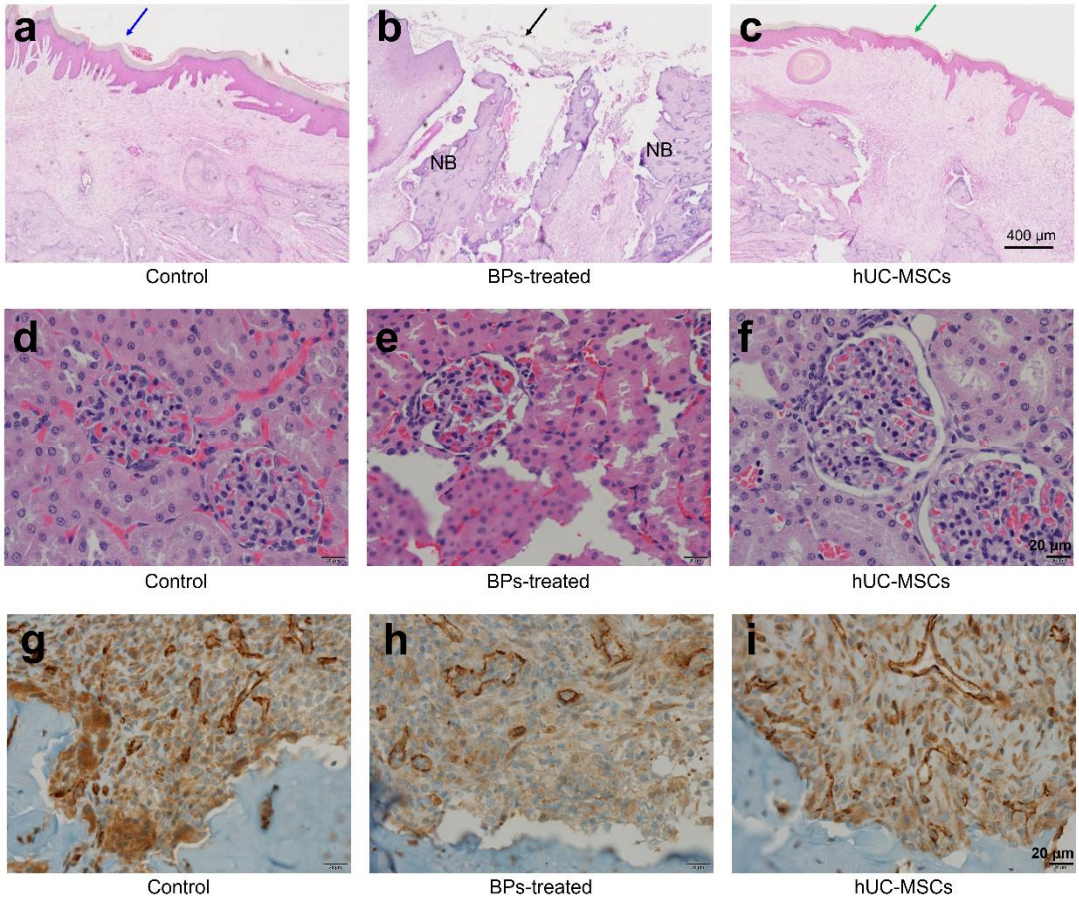

Fig. 6 Regeneration of the oral mucosal structure by hUC-MSCs at week 8. A–F H&E staining was used to examine the recovery of the overlying oral mucosal integrity induced by hUC-MSCs in the BRONJ-induced animal model are shown. In the BP-treated group, mucosal tissue structure was discontinuous and destroyed. However, in the hUC-MSC-transfused group, the overlying oral mucosa on the tooth extracted site was similar to that in the control group. **G–I** CD31 stain was used to examine the properties of damaged oral mucosal tissue and necrotic bone treatments, as indicators of renal vascular function. Compared to the other groups, CD31 showed an increased number of endothelial cells in the hUC-MSC group compared with the other groups. H&E stained images of the mucosa at the

tooth extracted sites. Natural healing (blue arrow) was seen in the control group (a). The BPs-treated group (black arrow) exhibited a destructed area on the mucosa (b); however, recovery was observed in the hUC-MSCs group (green arrow) (c). Scale bar, 400 uM

Discussion

The prevalence of BRONJ in patients with osteoporosis who are orally administered BPs is 1 in 1,262–4,419 (0.02–0.07%) [21]. For BP therapy administered via the intravenous route, the prevalence of BRONJ is increasing, and up to 0.017% of patients with osteoporosis and 1% of patients with cancer are diagnosed with BRONJ [22]. Currently, impaired activity of bone marrow stem cells (BMSCs), unbalanced bone metabolism, local inflammation with or without infection, and angiogenesis suppression are hypothesized to cause BRONJ [23]. Since MSCs have shown therapeutic potential on diverse diseases in previously studies, we hypothesized that MSCs potentially have applicability in treating and preventing causative factors of BRONJ by immune modulation and regenerative activity [24]. MSCs are not the same in terms of therapeutic potency, which varies according to the source of the MSCs. To date, MSCs from diverse tissue sources such as bone marrow, fat, blood, and umbilical cord have been isolated and studied. Although they share certain distinctive characteristics, MSCs from different sources also have unique characteristics. UC-MSCs obtained from umbilical cord Wharton's jelly have been highlighted as a useful resource with several merits compared to MSCs derived from other sources, such as BM-MSCs [25]. The advantages of UC-MSCs include ease of access, high expansion potential, and low immunogenicity because of their immaturity [18, 19]. Furthermore, compared to other types of MSCs, UC-MSCs are also known to have a stronger ability to differentiate into osteoblasts, which can play a major role in bone regeneration [20]. Consistent with our results, a recent study showed that the activities

of BMSCs derived from BRONJ lesions had decreased proliferative ability, self-renewal capacity, and multi differentiation capacity compared with control BMSCs. Osteoclast-inducing ability was also impaired in BRONJ BMSCs. All these results suggested that the decreased activities of BRONJ BMSCs might be an important factor leading to insufficient bone repair of BRONJ lesions [26]. A significant pathogenetic characteristic of BRONJ is the apoptosis of cells involved in bone metabolism. Nitrogen-containing BPs, such as zoledronate, alendronate, and pamidronate, can cause apoptosis in various cells, including osteoblasts and osteoclasts [17, 27]. Our data showed that BP-induced cell death can be suppressed by hUC-MSCs, which suggests that hUC-MSCs could be an effective treatment option for BRONJ. The anti-apoptotic effect of MSCs has been shown to be mediated by paracrine action, as confirmed by the separation of the explants in inserts or by supernatants from MSCs [28]. Our in vivo micro-CT analysis and H&E staining results demonstrated that intravenously transfused hUC-MSCs can heal BP-induced osteonecrosis of the jaw. The BRONJ induced animal models exhibited increased serum calcium and PTH levels, similar to those observed in secondary hyperparathyroidism (HPT); however, the hUC-MSC transfused BRONJ-induced animal models showed normalized PTH and calcium levels. Furthermore, the serum values of PTH and calcium in our study were similar to those observed in secondary HPT. The jawbone is affected by HPT, and brown tumor lesions in the jaw bone, observed with excess osteoclast activity, may be the earliest manifestation of this undiagnosed HPT in 6% of HPT cases [29]. Brown tumors are observed as osteolytic lesions that develop because of changes

in bone metabolism caused by high serum concentrations of PTH, which is very similar to the manifestations of BRONJ. Additionally, continuously upregulated PTH levels stimulate conventional T cells to secrete TNF-a, which augments Th17 cells, and in turn, stimulates them to secrete inflammatory factors such as RANKL, TNF-a, IL-1ß, and IL-6 [30]. Based on this, we suggest that renal dysfunction caused by BP treatment is not only the result of a parallel complication of BP treatment but also a significant cause of BRONJ. Further investigation is ongoing on this issue. According to Leizaola-Cardesa et al., BP-induced increases in serum PTH and calcium levels are normalized by transfused hUC-MSCs in the BRONJ-induced animal model [23, 31]. We speculate that the anti-inflammatory and regenerative effects on damaged organs, such as the kidney, can normalize the BP-induced upregulation of serum PTH and calcium levels by hUC-MSCs. Although further studies are needed to prove our hypothesis regarding HPT in patients with BRONJ, it is suggested that evaluation of PTH and calcium levels, as well as renal function, requires further investigation, due to the corresponding potential of progressing towards improved treatment protocols for patients with BRONJ. In many clinical cases, BRONJ starts from oral mucosal necrosis, where the mechanical stress is induced due to ill-fitting denture or other oral appliances. Recently Allam et al. investigated whether in vivo zoledronic acid (ZA) induces alterations in cell proliferation, apoptosis, and the expression of matrix metalloproteinases (MMPs) in oral mucosal epithelial cells. High doses of ZA resulted in higher levels of apoptosis and lower levels of MMP-9 in the oral epithelial cells, supporting the hypothesis that BP treatment affects

the oral mucosa [32]. In accordance with this result, our study showed that relatively more damaged oral mucosa with severe inflammation near the extraction socket was observed in the BRONJ group compared to the normal group. Consequently, regeneration of the damaged oral mucosa might delay healing and aggravate symptoms in the BRONJ group. However, Allam et al. reported that other mucosal areas looked intact, similar to the normal oral mucosa, consistent with our observations. Therefore, some surgical or mechanical stress might be essential for the progress of oral mucosal necrosis in BRONJ cases as bony necrosis progresses. Presently, infection is regarded as one of the key causes of BRONJ progression. According to a recent study, bacterial adhesion and biofilm formation are increased on denuded bone by BPs that act by lowering the pH of the exposed bony environment and inhibiting angiogenesis [33]. Also, microbial colonization was significantly increased in patients with BRONJ compared to that in patients with a necrotic bone of the jaw without a history of BP administration [34]. This increased microbial colonization on the denuded bone in patients at risk of BRONJ may support the use of antibiotics with a surgical treatment to prevent the development and aggravation of BRONJ. As MSCs can enhance hematopoiesis and anti-immune reactions, including mucosal regeneration [35], our results demonstrated that BRONJ-induced rats transfused with hUC-MSCs showed a more intact oral mucosal compared to that observed in the group not treated with hUC-MSCs. Therefore, it is clear that hUC-MSCs have therapeutic potential for the treatment of overlying mucosal tissue in BRONJ. Shifts in the RANKL/OPG ratio, in the context of bone tissue caused by BPs, are another

critical factor for BRONJ progression. In the current study, the RANKL/OPG ratio decreased slightly 2 d after treatment with the high dose of BPs, but at day 5, the RANKL/OPG ratio significantly increased. Recently, Koch et al. [36] suggested that the expression of OPG could initially be increased by BP administration but that the continuous administration of BPs further increases the expression level of RANKL. As a higher RANKL/OPG ratio could increase the number of osteoclasts at the defect site, we hypothesized that one of the mechanisms of BRONJ involved the necrosis of the denuded jawbone, facilitated by the increased number of osteoclasts after BP administration. This hypothesis may be supported by a previous study, in which patients with BRONJ showed increased numbers of osteoclasts expressing cysteine proteinase cathepsin K compared to the infected osteoradionecrosis- or control- group [37]. Additionally, in the current study, the shift in the RANKL/OPG ratio in rBM-derived cells after BP administration was normalized by the administration of hUC-MSCs. Although further investigation is required, the anti-inflammatory effect of hUC-MSCs might be a reason for the normalization of the RANKL/OPG ratio. In support of this hypothesis, in a previous study, pro-inflammatory cytokines were observed to upregulate the expression of RANKL, which facilitated the differentiation of inflammatory cells, including monocytes and macrophages, into osteoclasts [38]. The upregulation of osteogenic markers plays a crucial role in bone destructive diseases, including BRONJ. We also demonstrated that hUC-MSCs cultured with rBM-derived cells significantly enhanced the expression of osteogenic markers such as RUNX2, OSX, and BMP-2. RUNX2 and OSX are the transcription factors most

essential for the early stage of osteogenic differentiation. OSX is located downstream of RUNX2 and modulates osteoblastic differentiation rather than chondrogenesis [39, 40]. Moreover, BMP-2 is involved in osteogenic differentiation via ALP activity, promoting mineralization and upregulation of downstream osteogenic markers [41]. Thus, increased RUNX2, OSX, and BMP-2 expression induced by hUC-MSCs might play a key role in the synthesis of new bone in BRONJ. Severe local inflammation has been suggested to be another pathogenetic characteristic of BRONJ involved in the progression of the disease. Zhang et al. [42] suggested that inflammation resulting from the increase in IL-1ß caused by the BP-induced formation of the NLRP3/caspase-1 inflammasome aggravates the severity of BRONJ manifestation. Our in vitro results showed that inflammatory cytokines such as IL-1ß, IL-6, and TNF-a were increased by BP administration in rBM-derived cells and were restored to normal levels by hUC-MSC administration. Previous studies have reported that pro-inflammatory cytokines such as IL-1ß, IL-6, and TNF-a could play a role in attracting inflammatory cells to the inflammatory site [43, 44]. Our results confirmed that hUC-MSCs downregulated the aforementioned cytokines. In this study, the successful xenograft implanted using hUC-MSCs in a rat model might be notable evidence of the low immunogenicity of hUC-MSCs. Several studies have already shown that hUC-MSCs demonstrate a therapeutic effect in Parkinson's disease, acute lung injury, and acute hepatic necrosis in other species [10–12]. This characteristic of hUC-MSCs suggests that they will potentially be applicable for use in future allogenic trials in human clinical cases. In conclusion, this study demonstrated,

directly or indirectly, that hUC-MSCs have potential as therapeutic agents for BRONJ in vitro and in vivo. The hUC-MSCs inhibited BP-induced inflammatory responses and enhanced the expression of osteogenic factors, including RUNX2, OSX, and BMP-2, in vitro. Furthermore, we confirmed the normalization of RANKL/OPG expression levels as final markers affecting bone homeostasis by hUC-MSCs. We also developed a BRONJ-induced animal model and showed that hUC-MSCs transfusion could improve bone repair in this model. Therefore, we suggest that hUC-MSCs might be a crucial therapeutic agent for BRONJ treatment.

References

1. Kim, J., et al., *Bisphosphonate-related osteonecrosis of the jaw: Current clinical significance and treatment strategy review.* Am J Dent, 2020. **33**(3): p. 115-128.
2. Silverman, S.L. and R. Landesberg, *Osteonecrosis of the jaw and the role of bisphosphonates: a critical review.* The American journal of medicine, 2009. **122**(2): p. S33-S45.
3. Bagan, J., et al., *Osteonecrosis of the jaws in patients treated with intravenous bisphosphonates (BRONJ): A concise update.* Oral oncology, 2009. **45**(7): p. 551-554.
4. Agrillo, A., et al., *Bisphosphonate-related osteonecrosis of the jaw (BRONJ): 5 year experience in the treatment of 131 cases with ozone therapy.* Eur Rev Med Pharmacol Sci, 2012. **16**(12): p. 1741-7.
5. Fliefel, R., et al., *Treatment strategies and outcomes of bisphosphonate-related osteonecrosis of the jaw (BRONJ) with characterization of patients: a systematic review.* International journal of oral and maxillofacial surgery, 2015. **44**(5): p. 568-585.
6. Rosella, D., et al., *Medication-related osteonecrosis of the jaw: Clinical and practical guidelines.* Journal of International Society of Preventive & Community Dentistry, 2016. **6**(2): p. 97.
7. Shin, S.-H., et al., *Effect of low-level laser therapy on bisphosphonate-treated osteoblasts.* Maxillofacial plastic and reconstructive surgery, 2016. **38**(1): p. 1-8.
8. Kaibuchi, N., et al., *Multipotent mesenchymal stromal cell sheet therapy for bisphosphonate-related osteonecrosis of the jaw in a rat model.* Acta biomaterialia, 2016. **42**: p. 400-410.
9. Friedenstein, A., F. AJ, and P. AF, *Precursors for fibroblasts in different populations of hematopoietic cells as detected by the in vitro colony assay method.* 1974.
10. Shi, L.-L., F.-P. Liu, and D.-W. Wang, *Transplantation of human umbilical cord blood mesenchymal stem cells improves survival rates in a rat model of acute hepatic necrosis*. The American journal of the medical sciences, 2011. **342**(3): p. 212-217.

11. Zhu, H., et al., *Therapeutic effects of human umbilical cord-derived mesenchymal stem cells in acute lung injury mice.* Scientific reports, 2017. **7**(1): p. 1-11.
12. Mathieu, P., et al., *Neuroprotective effects of human umbilical cord mesenchymal stromal cells in an immunocompetent animal model of Parkinson's disease.* Journal of neuroimmunology, 2012. **246**(1-2): p. 43-50.
13. Rachakatla, R.S., et al., *Combination treatment of human umbilical cord matrix stem cell-based interferon-beta gene therapy and 5-fluorouracil significantly reduces growth of metastatic human breast cancer in SCID mouse lungs.* Cancer investigation, 2008. **26**(7): p. 662-670.
14. Boomsma, R.A., P.D. Swaminathan, and D.L. Geenen, *Intravenously injected mesenchymal stem cells home to viable myocardium after coronary occlusion and preserve systolic function without altering infarct size.* International Journal of Cardiology, 2007. **122**(1): p. 17-28.
15. Matsuura, Y., et al., *Therapeutic interactions between mesenchymal stem cells for healing medication-related osteonecrosis of the jaw.* Stem cell research & therapy, 2016. **7**(1): p. 1-11.
16. Li, Y., et al., *Allogeneic mesenchymal stem cell therapy for bisphosphonate-related jaw osteonecrosis in swine.* Stem cells and development, 2013. **22**(14): p. 2047-2056.
17. Ogata, K., et al., *Evaluation of the therapeutic effects of conditioned media from mesenchymal stem cells in a rat bisphosphonate-related osteonecrosis of the jaw-like model.* Bone, 2015. **74**: p. 95-105.
18. Weiss, M.L., et al., *Immune properties of human umbilical cord Wharton's jelly-derived cells.* Stem cells, 2008. **26**(11): p. 2865-2874.
19. Prasanna, S.J., et al., *Pro-inflammatory cytokines, IFNγ and TNFα, influence immune properties of human bone marrow and Wharton jelly mesenchymal stem cells differentially.* PloS one, 2010. **5**(2): p. e9016.
20. Malgieri, A., et al., *Bone marrow and umbilical cord blood human mesenchymal stem cells: state of the art.* International journal of clinical and experimental medicine, 2010. **3**(4): p. 248.

21. Kim, H., et al., *Therapeutic effect of mesenchymal stem cells derived from human umbilical cord in rabbit temporomandibular joint model of osteoarthritis.* Scientific reports, 2019. **9**(1): p. 1-14.

22. Tanna, N., et al., *Awareness of medication related osteonecrosis of the jaws (MRONJ) amongst general dental practitioners.* British dental journal, 2017. **222**(2): p. 121-125.

23. Ruggiero, S.L., et al., *American Association of Oral and Maxillofacial Surgeons position paper on medication-related osteonecrosis of the jaw—2014 update.* Journal of oral and maxillofacial surgery, 2014. **72**(10): p. 1938-1956.

24. Ribatti, D., et al., *Neridronate inhibits angiogenesis in vitro and in vivo.* Clin Rheumatol, 2007. **26**(7): p. 1094-8.

25. Wang, Y., et al., *Mesenchymal stem cell-derived secretomes for therapeutic potential of premature infant diseases.* Biosci Rep, 2020. **40**(5).

26. Eliane, G., et al., *Hematopoietic reconstitution in a patient with Fanconi''s anemia by means of umbilical-cord blood from an HLA-identical sibling (1989).* Cellular Therapy and Transplantation, 2011. **2**(3 (7)).

27. He, L.H., et al., *Role of Bone Marrow Stromal Cells in Impaired Bone Repair from BRONJ Osseous Lesions.* J Dent Res, 2017. **96**(5): p. 539-546.

28. Manzano-Moreno, F.J., et al., *High doses of bisphosphonates reduce osteoblast-like cell proliferation by arresting the cell cycle and inducing apoptosis.* Journal of Cranio-Maxillofacial Surgery, 2015. **43**(3): p. 396-401.

29. Kossl, J., et al., *Anti-Apoptotic Properties of Mesenchymal Stem Cells in a Mouse Model of Corneal Inflammation.* Stem Cells Dev, 2021.

30. Mittal, S., et al., *Oral manifestations of parathyroid disorders and its dental management.* Journal of Dental and Allied Sciences, 2014. **3**(1): p. 34.

31. Li, J.-Y., et al., *IL-17A is increased in humans with primary hyperparathyroidism and mediates PTH-induced bone loss in mice.* Cell metabolism, 2015. **22**(5): p. 799-810.

32. Leizaola-Cardesa, I.-O., et al., *Bisphosphonates, vitamin D, parathyroid hormone, and osteonecrosis of the jaw. Could there be a missing link?* Medicina oral, patología oral y cirugía bucal, 2016. **21**(2): p. e236.

33. Allam, E., et al., *In vivo effects of zoledronic acid on oral mucosal epithelial cells.* Oral Dis, 2011. **17**(3): p. 291-7.

34. Kos, M., et al., *Bisphosphonates enhance bacterial adhesion and biofilm formation on bone hydroxyapatite.* Journal of Cranio-Maxillofacial Surgery, 2015. **43**(6): p. 863-869.

35. Kos, M., et al., *Clinical comparison of patients with osteonecrosis of the jaws, with and without a history of bisphosphonates administration.* International journal of oral and maxillofacial surgery, 2010. **39**(11): p. 1097-1102.

36. Pettersson, L.F., et al., *In vitro osteogenic differentiation of human mesenchymal stem cells from jawbone compared with dental tissue.* Tissue engineering and regenerative medicine, 2017. **14**(6): p. 763-774.

37. Koch, F.P., et al., *Influence of bisphosphonates on the osteoblast RANKL and OPG gene expression in vitro.* Clinical oral investigations, 2012. **16**(1): p. 79-86.

38. Hansen, T., et al., *Increased numbers of osteoclasts expressing cysteine proteinase cathepsin K in patients with infected osteoradionecrosis and bisphosphonate-associated osteonecrosis—a paradoxical observation?* Virchows Archiv, 2006. **449**(4): p. 448-454.

39. Nakashima, T. and H. Takayanagi, *Osteoimmunology: crosstalk between the immune and bone systems.* Journal of clinical immunology, 2009. **29**(5): p. 555.

40. Nakashima, K., et al., *The novel zinc finger-containing transcription factor osterix is required for osteoblast differentiation and bone formation.* Cell, 2002. **108**(1): p. 17-29.

41. Heino, T.J. and T.A. Hentunen, *Differentiation of osteoblasts and osteocytes from mesenchymal stem cells.* Current stem cell research & therapy, 2008. **3**(2): p. 131-145.

42. Sun, J., et al., *Role of bone morphogenetic protein-2 in osteogenic differentiation of mesenchymal stem cells.* Molecular medicine reports, 2015. **12**(3): p. 4230-4237.

43. Zhang, Q., et al., *Bisphosphonate induces osteonecrosis of the jaw in diabetic mice via NLRP3/Caspase-1-dependent IL-1β mechanism.* Journal of Bone and Mineral Research, 2015. **30**(12): p. 2300-2312.

44. Sauty, A., et al., *Interleukin-6 and tumor necrosis factor α levels after bisphosphonates treatment in vitro and in patients with malignancy.* Bone, 1996. **18**(2): p. 133-139.

45. Melcher, M., et al., *Modulation of oxidative phosphorylation and redox homeostasis in mitochondrial NDUFS4 deficiency via mesenchymal stem cells.* Stem cell research & therapy, 2017. **8**(1): p. 1-14.

국문 요약

배경 및 목적: 골다공증, 다발성골수염, 악성종양의 골전이, 암 환자의 과칼슘혈증 등의 치료를 위해 광법위하게 사용 되는 비스포스포네이트 계열 약물은 장기간 사용 시 심각한 골대사의 불균형을 초래하고 그로인해 턱뼈괴사증(BRONJ)을 비롯한 다양한 합병증을 유발시킨다. 최근 연구에 따르면 중간엽 줄기세포는 항염증 및 조직재생에 효과가 있는것으로 알려져있으며, 본 연구에서는 앞서 언급한 효과가있는 중간엽줄기세포를 활용하여 턱뼈괴사증에 대한 치료 효과를 in-vitro와 in-vivo모델을 통하여 확인 하였다.

연구재료 및 연구방법: 본 연구에서는 랫드의 골수유래세포를 활용하여 cell viability, colony-forming, real-time PCR 및 FACS 기법을 활용하여 염증인자 및 뼈재생 마커들의 발현정도를 통해 in vitro상에서 hUC-MSCs가 골대사 질환에서 효과가 있는지를 탐색하였다. 또한, micro-CT, H&E 염색, IHC 염색, 및 ELISA기법을 활용하여 비스포스포네이트에 의해 유도된 턱뼈괴사증 동물모델을 통해 hUC-MSCs의 치료효과를 in vivo상에서 검증하였다.

연구결과: 비스포스포네이트에 의해 유도된 랫드의 골수유래 세포의 세포독성 및 염증반응이 hUC-MSCs에 의해 감소되었고, RUNX2, OSX, BMP-2등의 뼈재생 마커들의 발현이 hUC-MSCs에 의해 확연히 증가한 것을 확인하였다. 또한, 비스포스포네이트에 의해 왜곡된 RANKL/OPG의 발현 비율이 hUC-MSCs의

co-culture에 의해 교정되는 것을 확인하였다. 이러한 in vitro의 결과와 일치하게 턱뼈괴사증 동물모델에서 비스포스포네이트에 의한 점막의 손상과 질환부위의 뼈괴사가 hUC-MSCs의 투여로인해 감소한것이 관찰되었고, 비스포스포네이트에 의한 심각한 신장손상 및 PTH와 혈중 Ca농도 변형이 hUC-MSCs에 의해 완화되는 것을 확인하였다.

결론: 본 연구결과, 인간 제대조직 유래 줄기세포가 턱뼈괴사증 질병 치료를 위한 효과적인 치료제가 될 수 있음을 확인하였다.